

# Evaluating the green potential and optimizing strategies for two industrial brownfields in Harbin, China

Cui J<sup>1</sup>, Jia Z-Y<sup>2</sup> and Zhang Y-H<sup>2\*</sup>

<sup>1</sup>School of Architecture and Civil Engineering, Faculty of Science, Engineering and Technology, University of Adelaide, Australia

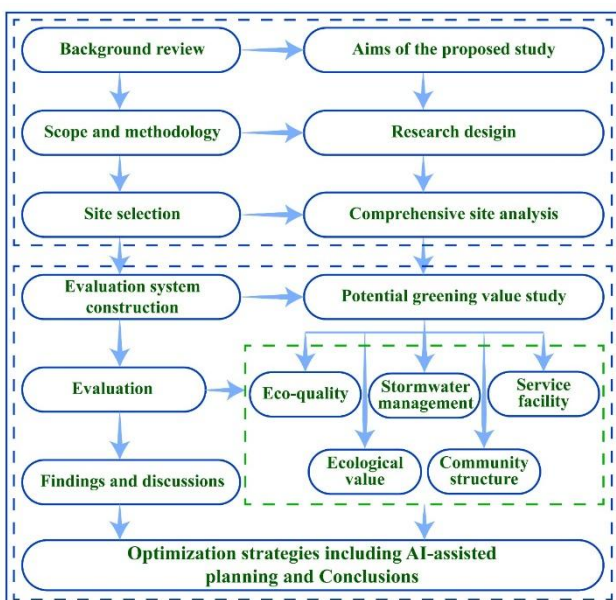
<sup>2</sup>M-Grass Ecology and Environment (Group) Co., Ltd, Hohhot, China

Received: 20/10/2025, Accepted: 27/12/2025, Available online: 09/01/2026

\*to whom all correspondence should be addressed: e-mail: pp7768@126.com

<https://doi.org/10.30955/gnj.08121>

## Graphical abstract



## Abstract

With the upgrading of urban industrial structures, the regenerative use of industrial wasteland has become vital for sustainable urban renewal. Transforming such sites into green spaces can alleviate urban green space shortages and improve ecological quality. This study focuses on two distinct industrial wasteland sites in Harbin's Xiangfang District, namely the former Xingguang Machinery Factory (XMF) and the former Textile Printing and Dyeing Factory (TPDF). A green value evaluation system comprising five criterion layers and 21 indicators was established using the Analytic Hierarchy Process (AHP), and field surveys and GIS analysis were applied for assessment. The results indicate that XMF (score 3.76) exhibits significantly higher green value than TPDF (score 2.44), mainly due to differences in ecological quality, pollution levels, and urban integration. Differentiated regeneration strategies incorporating AI-assisted planning (e.g., machine learning for contamination mapping and

generative design for spatial configuration) are proposed. For XMF, an ecology-culture integrated park is recommended, while for TPDF, an art-led green cultural-creative district with zoned remediation is suggested. This research offers a scientifically supported and technology-informed approach for the sustainable regeneration of industrial wasteland.

**Keywords:** industrial brownfield, green value evaluation, analytic hierarchy process (AHP); landscape optimization strategy, Harbin

## 1. Introduction

Rapid urbanization and the advent of the post-industrial era have led to the emergence of numerous industrial wastelands within cities (Accordino & Johnson 2000). The formation of these sites results from the interplay of various complex factors, including global and local economic changes, climatic conditions, social structure, political decisions, population movements, and cultural context (Cui *et al.* 2025; Hwang & Lee 2019; Mrak *et al.* 2022; Newman *et al.* 2018). During industrial transformation and urban renewal, numerous brownfields and abandoned plots have emerged as legacy spaces that cannot be overlooked in urban development (Chien & Knoble 2024; Qu *et al.* 2020; Song *et al.* 2020).

These areas not only face problems such as soil pollution, ecological degradation, and landscape fragmentation (Adams *et al.* 2010), but also fragment the city's physical structure and visual landscape to some extent, while harboring environmental pollution and public safety risks that pose potential threats to residents' lives (Beam *et al.* 2021; Cui *et al.* 2022; Cundy *et al.* 2016). However, from the perspective of urban ecological restoration, these brownfield resources, often seen as "urban scars", can be transformed into important catalysts for urban vitality. Their conversion into urban green spaces can bring profound impacts for sustainable urban development (Anderson & Minor 2017; Preston *et al.* 2024; Rupprecht & Byrne 2014; Stanford *et al.* 2025). This transformation is significant for alleviating construction land shortages,

improving residents' quality of life, and preserving industrial culture (Adams *et al.* 2010).

In recent years, researchers and practitioners worldwide have continuously explored diverse regeneration strategies including ecological restoration, landscape remodeling, and functional replacement, while introducing cutting-edge technologies such as artificial intelligence to enhance the scientific rigor and foresight of industrial wasteland redevelopment (Mao *et al.* 2022; Naghibi *et al.* 2021; Song *et al.* 2022; Xi 2024). However, current research predominantly focuses on overall transformation models or discussions of single cases, while comparative studies examining the inherent characteristics and differences in greening potential among different types of industrial wasteland remain insufficient (Derudder & Taylor 2021; Fu *et al.* 2024). Particularly, wastelands originating from different industrial sectors (e.g., heavy industry vs. light industry) exhibit essential differences in historical context, spatial structure, pollution levels, and other aspects, which inevitably lead to differentiation in their green value and regeneration pathways (Draus *et al.* 2020; Gobster *et al.* 2020; Hsiao 2022). Current research on evaluation systems and differentiated strategies for urban wasteland utilization requires further enhancement (Cui *et al.* 2025). How to scientifically evaluate greening potential and formulate targeted landscape optimization strategies has become a research hotspot in fields such as landscape architecture, urban and rural planning, and urban ecology (Akkerman & Cornfeld 2009; Atkinson *et al.* 2014; Cady *et al.* 2020; Chen & Hashimoto 2025).

Against the backdrop above, a key scientific question arises: Do brownfields originating from different industrial sectors exhibit significantly different green potentials, and which ecological or social factors primarily drive these differences? To address this, it is necessary to move beyond established ecosystem service-based or ecological security pattern models (e.g., Cundy *et al.* 2016; Atkinson *et al.* 2014). This study aims to develop a novel green value evaluation system that integrates and weighs sector-specific factors (such as legacy pollution level, landscape structural adaptability, and cultural-historical value) with multi-dimensional urban integration indicators. This approach seeks to capture the distinct greening constraints and opportunities inherent to different industrial histories, thereby offering a more nuanced tool for comparative potential assessment and differentiated strategy formulation.

Harbin, China, as a typical representative of China's old industrial base, has the rise and fall of industrial civilization deeply imprinted in its urban fabric. Xiangfang District, located in the southeast of the city, served not only as a pioneering area for industrialization in Northeast China but also accumulated a large number of different types of industrial heritage and wasteland during the tides of the era. This study selects two highly contrasting typical cases within this region. The first is the former Xingguang Machinery Factory (XMF), which was military-industrial in nature with sturdy and grand buildings and relatively

singular pollution. The second is the former Textile Printing and Dyeing Factory (TPDF), which was involved in textile printing and dyeing with lighter buildings but complex and severe pollution. This stark contrast between "hard and soft", "heavy and light" provides an excellent sample for addressing the research question.

Building on the proposed evaluation framework, this paper aims to quantitatively analyze the differences in greening potential between the two sites. Through site visits, questionnaires, field investigations, expert evaluations, and the Analytic Hierarchy Process (AHP) method, a comprehensive assessment of the greening potential of the two sites was conducted. Based on the evaluation results, this study proposes landscape optimization strategies matching their respective characteristics, aiming to provide a scientifically supported and differentiated approach for ecological restoration and landscape regeneration of similar industrial wastelands.

## 2. Materials and methods

### 2.1. Study area overview

Harbin (45°40'- 48°40'N, 125°40'-130°10'E) is located in Northeast China, the capital of Heilongjiang province, situated in the middle reaches of the Songhua River (You 2024). The total area of Harbin is about 53,000 km<sup>2</sup>, making it one of the provincial capitals with the largest area in China (Xu and Xu 2020). Harbin was once a key industrial base constructed in the early years of the People's Republic of China. Through the 'Southern Factory Relocation North' and the layout of several national major projects, it gradually formed an industrial system supported by large and medium-sized state-owned enterprises and covering comprehensive categories. Its power station equipment, precision bearings, military products, etc., were at the forefront of the country in terms of technical capability and industrial scale, becoming an important force driving national industrialization and regional economic growth (Zhang *et al.* 2023). The heavy industrial bases in the early founding period were mainly located in the Xiangfang District in the southeast of Harbin (Ge 2017), as shown in **Figure 1**.

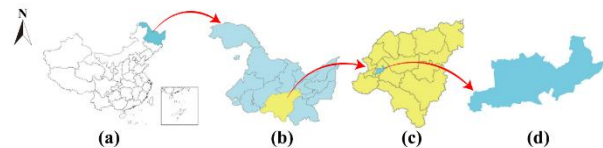


**Figure 1.** Location Map of Xiangfang District, Harbin City. (a) Outline Map of China; (b) Outline Map of Heilongjiang Province; (c) Outline Map of Harbin City; (d) Outline Map of Xiangfang District.

With the advancement of the market economy transition in recent years, the traditional industrial structure long relied upon by Harbin struggled to adapt to diversified demands, and many enterprises faced challenges of overcapacity and lagging technological upgrades. Against the backdrop of urban functional adjustment and industrial relocation, many old factory sites were successively closed, relocated, or transformed, with the

original sites gradually turning into residential and commercial land. For example, the original Linen Factory, Cement Factory, and other plots have been developed into new urban functional areas. Simultaneously, some factory buildings have been preserved and transformed into cultural and creative parks or commercial spaces, becoming typical cases of industrial heritage reuse. In this process, a considerable number of old factory areas have been left idle and abandoned for various reasons, forming a considerable scale of industrial wasteland, such as the concentrated abandoned factory areas of bearing factories, timber factories, chemical plants, machinery factories, silk spinning mills, and textile printing and dyeing factories in Xiangfang District. These sites not only affect land value and the urban environment but also reflect the growing pains of regional industrial structure adjustment.

Based on the identification of wasteland in Harbin's Xiangfang District using high-resolution satellite imagery (Gaofen-6) combined with ArcGIS 10.8, along with preliminary field surveys assisted by drone technology (DJI Goggles 2), this study selected two distinct types of industrial wasteland, namely the former military-industrial Xingguang Machinery Factory (XMF) and the former textile printing and dyeing factory (TPDF), for research on differences in greening potential (Figure 2).

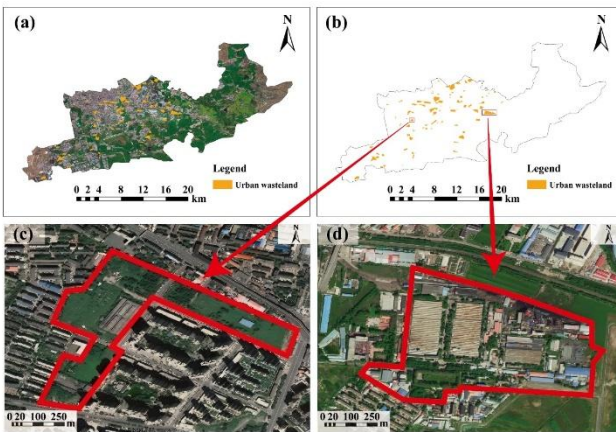


**Figure 2.** Geographical Context and Satellite Imagery of the XMF and TPDF Industrial Wasteland Sites. (a) and (b): Locator maps showing the position of the sites within Xiangfang District; (c) and (d): High-resolution satellite image overviews of the XMF and TPDF sites, respectively.

XMF was established in 1965, as a military enterprise directly under the former Ministry of Aerospace Industry. The site area is 21.22 hectares. Some internal factory buildings have been demolished, but the core protective buildings are relatively intact. The green coverage rate is high, reaching 84.91%, and vegetation growth is good. Pollution sources are mainly heavy metals and lubricating oil from machining. TPDF was built in the 1980s, as a comprehensive textile enterprise. The site area is 49.60 hectares. Most of the internal factory structures remain, but there is a lot of hardened ground. Pollution mainly comes from dyes, auxiliaries, and organic wastewater from the printing and dyeing process, with complex composition and high treatment difficulty. The green coverage rate is low, only 32.01%. Aerial photographs of

the two wasteland sites are shown in Figure 3; they were acquired in June 2024.



**Figure 3.** Aerial photographs of the XMF and TPDF industrial wasteland sites. (a1-a4) The XMF site, shown from different viewing angles; (b1-b4) The TPDF site, shown from different viewing angles. The area enclosed by the red line demarcates the extent of the factory premises, with the area beyond it defined as the surrounding zone.

## 2.2. Construction of the green value evaluation system

This study employed the Analytic Hierarchy Process (AHP) to construct the evaluation system (Byun 2001). The goal layer (A) is Green Value. The criterion layer (B) consists of five aspects: Eco-quality (B1), Ecological Value (B2), Stormwater Management (B3), Community Structure (B4), and Service Facilities (B5). The indicator layer (C) includes 21 specific indicators, such as Vegetation Coverage (C1), Original Site Area (C6), Water Retention Potential (C10), Community Utilization Potential (C15), Transportation Services (C17), etc. The hierarchical structure model of the green value evaluation system is detailed in Figure 4.

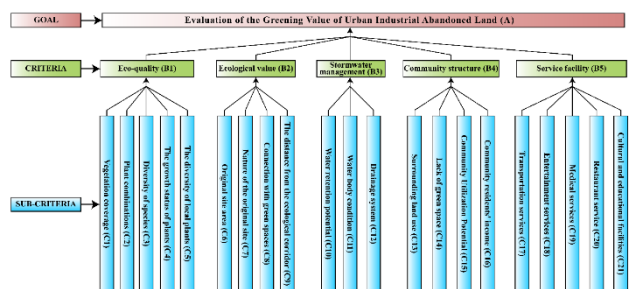


**Figure 4.** Analytic Hierarchy Process (AHP) model for evaluating the green value of industrial wasteland.

## 2.3. Procedure of Consultation and Questionnaire Administration

A panel of experts specializing in landscape architecture, urban planning, and architectural engineering was

assembled (see **Supplementary Table 1**). Expert selection criteria included: holding an associate senior professional title or above, having over 10 years of research or practical experience in related fields, and possessing hands-on project experience in industrial heritage regeneration or ecological restoration. The expert panel conducted pairwise comparisons of indicators through a combination of field visits and structured interviews to construct judgment matrices.

A total of 200 questionnaires were distributed to residents surrounding each site, resulting in 368 valid responses, representing a response rate of 92%. The demographic profile of respondents was as follows: the majority (62%) were aged 30-50, most (71%) held a college degree or higher, and occupations included employees of enterprises and institutions, self-employed individuals, students, and retirees. Respondents rated the importance of the 21 specific indicators using a 5-point Likert scale (1-5).

**Table 1.** Weights and ranking of green potential evaluation for each criteria

A	B1	B2	B3	B4	B5	Wi	Order
B1	1	0.2703	3.8912	3.1436	2.1748	0.2242	2
B2	3.7037	1	4.9206	3.9603	4.0315	0.4597	1
B3	0.2571	0.2033	1	0.2924	0.3618	0.0556	5
B4	0.3185	0.2525	3.4483	1	2.8624	0.1575	3
B5	0.4608	0.2481	2.7778	0.3497	1	0.1030	4

*Note: The meanings of each code as shown in Figure 4.*

## 2.5. Model Validation and Sensitivity Analysis

To assess the robustness of the evaluation model, a sensitivity analysis was conducted. Weights at the criterion level were randomly varied within a range of  $\pm 10\%$  to observe their impact on the total green value scores. Results indicated that under these weight fluctuations, the green value levels of the two study sites remained stable. This demonstrates the model's reliability and the credibility of the evaluation outcomes. Furthermore, the questionnaire survey results of this study also confirmed the stability of the model.

## 2.6. Data Sources and Processing

Data sources include the following aspects: (1) High-resolution satellite imagery (Gaofen-6) from 2022, and aerial imagery (DJI Goggles 2) from 2024; (2) Experts field survey and vegetation quadrat survey; (3) Relevant urban planning documents and GIS database of Xiangfang District; (4) Residents questionnaire survey.

Scores for each indicator were quantified based on pre-established scoring criteria (**Supplementary Table 2**, **Table 3**, **Table 4**, **Table 5**, **Table 6**). Statistical significance of differences between groups was determined using the Student's t-test (Barrado *et al.* 2016), and associations between variables were assessed by Pearson correlation analysis (Mo *et al.* 2025).

## 2.7. Comprehensive Evaluation Model

The comprehensive index evaluation method was used to calculate the total green value score (A), with the formula as follows:

## 2.4. Weight Determination and Consistency Check

The geometric mean method was applied to aggregate data from expert judgment matrices and resident questionnaires to calculate the weights of indicators at each level. All judgment matrices passed the consistency check, with Consistency Ratio (CR) values as follows: 0.043 (Criterion layer A), 0.028 (Eco-quality B1), 0.036 (Ecological value B2), 0.021 (Stormwater management B3), 0.039 (Community structure B4), and 0.031 (Service facilities B5).

All CR values were below 0.1, satisfying the consistency requirement. Final weights and rankings are presented in **Table 1**. The weight analysis revealed that Ecological Value (B2) and Eco-quality (B1) are the most critical factors determining green value, ranking first and second, respectively.

$$A = \sum (B_i \times W_i)$$

Here,  $B_i$  is the score of the  $i$ -th criterion layer, and  $W_i$  is its corresponding weight. The criterion layer score  $B_i$  is obtained by the weighted sum of its subordinate indicator layer scores. Scores are given on a 5-point scale (1, 2, 3, 4, 5). The value is categorized as follows: 'Low' for scores in the [1-2] range, 'Medium' for [2-3], 'High' for [3-4], and 'Very High' for [4-5].

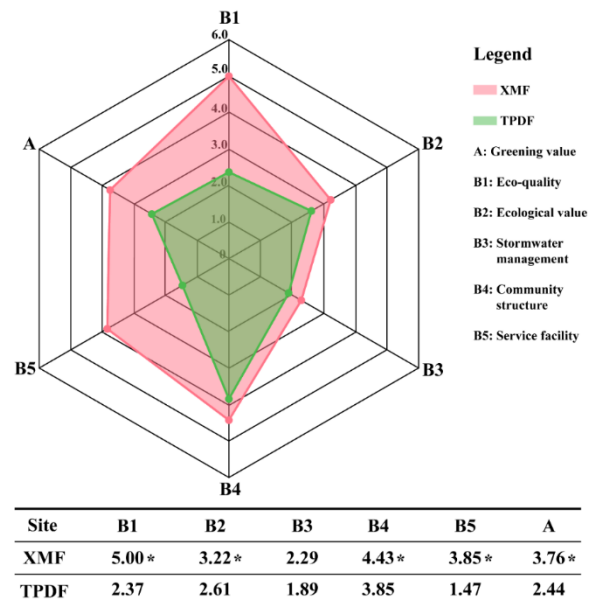


**Figure 5.** Comparison of Green Value Evaluation Scores between the XMF and TPDF Sites. \* indicates a significant differences between XMF and TPDF ( $p < 0.05$ ).

### 3. Results and Analysis

#### 3.1. Comprehensive Green Value Evaluation Results

According to the comprehensive evaluation model calculation, the total green value scores and various criterion layer scores for the XMF and TPDF sites are shown in **Figure 5**.

The **Figure 5** showed that all scores of different criteria layers in XMF were higher than in TPDF. And also the total green value score of the XMF (3.76) is significantly higher than that of the TPDF site (2.44). This indicates that, in **Table 2**, Score and weight of each sub-criteria for calculating greening value (B1 to B5)

Sub-criteria	Score in XMF	Score in TPDF	Weight	Sub-criteria	Score in XMF	Score in TPDF	Weight
C1	5	2	0.0801	C12	1	5	0.0124
C2	5	4	0.0096	C13	5	5	0.0746
C3	5	3	0.0351	C14	3	2	0.0108
C4	5	4	0.0146	C15	5	2	0.0495
C5	5	2	0.0848	C16	2	5	0.0225
C6	4	5	0.1826	C17	4	2	0.0481
C7	2	1	0.1965	C18	4	1	0.0168
C8	5	1	0.0484	C19	4	1	0.0056
C9	3	1	0.0322	C20	4	1	0.0167
C10	3	1	0.0359	C21	3	1	0.0159
C11	1	1	0.0073				

The total scores of XMF and TPDF of Eco-quality (B1) in **Figure 5** calculated based on the comprehensive index evaluation formula that mentioned before, combining with the scores in **Table 2** and the weights in **Supplementary Table 2**. The processing are as follows:

$$XMF = 5 * 0.36 + 5 * 0.04 + 5 * 0.16 + 5 * 0.07 + 5 * 0.38 = 5.00$$

$$TPDF = 2 * 0.36 + 4 * 0.04 + 3 * 0.16 + 4 * 0.07 + 2 * 0.38 = 2.37$$

Also the total scores in Ecological Value (B2), Stormwater Management (B3), Community Structure (B4) and Service Facilities (B5) following the same processing above based on **Table 2** and **Supplementary Tables 3-6**.

To go beyond the earlier descriptive disparities, a Pearson correlation analysis of the combined sites' standardized scores (B1-B5) is conducted here. Results revealed a strong positive correlation between Eco-quality (B1) and Stormwater Management (B3) ( $r = 0.89$ ,  $p < 0.01$ ), indicating that sites with better inherent ecological conditions (e.g., higher vegetation cover) inherently possess greater potential for stormwater retention that is a synergy evident in XMF's superior performance in both aspects. Furthermore, a significant positive correlation was found between Community Structure (B4) and Service Facilities (B5) ( $r = 0.92$ ,  $p < 0.01$ ), underscoring that well-integrated urban neighborhoods are typically accompanied by more complete service infrastructures, as seen in the XMF context.

To move beyond description towards causal explanation, the analysis explicitly links indicator scores to the sites' industrial typology. The stark contrast in Eco-quality (B1), where XMF (5.00) vastly outperformed TPDF (2.37), is directly attributable to their original industrial footprints.

terms of comprehensive potential for transformation into green space, the Xingguang Machinery Factory is superior to the Textile Printing and Dyeing Factory.

#### 3.2. Comparative and Correlative Analysis of Greening Values

To elucidate the underlying causes of the differences in total green value, a detailed comparison across the five criterion layers was conducted (**Figure 5**). The scores and weighted contributions of each sub-criterion (C1 - C21) are presented in **Table 2**.

**Table 2.** Score and weight of each sub-criteria for calculating greening value (B1 to B5)

XMF, as a machinery factory, had extensive interstitial land which underwent natural succession after abandonment, leading to high scores in vegetation coverage (C1) and local plant diversity (C5). Conversely, TPDF's textile printing and dyeing operations required large areas of hardened ground for logistics and wastewater treatment, resulting in a legacy of low vegetation coverage and a compromised ecological baseline.

The divergence in Ecological value (B2) is fundamentally driven by pollution intensity. XMF's operations involved localized contaminants like heavy metals. In contrast, TPDF's use of complex dyes and organic compounds led to widespread, severe contamination. This intrinsic difference in pollution burden is a primary constraint on TPDF's ecological recovery potential. Additionally, XMF's superior 'Connection to green spaces' (C8) score is not incidental but relates to its historical siting within a planned industrial zone near other facilities with green buffers, enhancing urban ecological connectivity.

The assessment of Stormwater management (B3) further validates the link between industrial legacy and ecosystem function. The high score in XMF is directly tied to its superior vegetation coverage (C1), which promotes infiltration, despite both sites having poor underlying permeability due to industrial compaction.

Finally, the chasm in Community structure (B4) and Service facilities (B5) finds its root in the original locational logic of each industry. XMF, as a key state-owned enterprise, was integrated into a well-serviced urban district from its inception, leading to high surrounding population density (C15) and complete services (C17). TPDF, with needs for water access and effluent disposal,

was historically situated on the urban fringe. Subsequent urban growth has not fully integrated this area, leaving it with lower community density and a critical lack of services, thereby limiting its immediate social utility and accessibility.

However, the above statistical and correlational analyses also have certain limitations. Although two cases are strategically selected for their contrasting typologies, the small sample size and locations limit the generalizability of the statistical correlations observed. Future work should expand the number of sites across multiple cities to strengthen the robustness of the evaluation framework and the derived inter-indicator relationships.

#### 4. Discussion

##### 4.1. Underlying Reasons for Differences in Green Value

It should be noted that industrial wastelands in different regional and urban contexts often possess uniqueness in their historical background, spatial characteristics, and social and cultural significance. Therefore, deeply interpreting their formation context and landscape morphology not only helps understand their local value but also provides key perspectives and methodological support for formulating more adaptive and humanistic regeneration strategies (Beames *et al.* 2018; Li *et al.* 2018; Li *et al.* 2024; Preston *et al.* 2023). The two case studies selected show prominent differences in green utilization value.

The comprehensive green value score of the XMF site (3.76) was substantially higher than that of the TPDF site (2.44), indicating a significant disparity in their potential for transformation into urban green space. This divergence stems directly from their distinct original industrial attributes, which have profoundly shaped their current ecological conditions, pollution status, and urban integration, as quantified in the evaluation results across the five criterion layers.

First, the stark contrast in Eco-quality (B1), where XMF (5.00) vastly outperformed TPDF (2.37), is primarily attributable to their differing industrial footprints and subsequent ecological disturbance. The XMF site, as a machinery factory, featured large, impervious factory buildings but also extensive interstitial land. After its abandonment, this land experienced minimal ongoing disturbance, allowing for natural succession. This is evidenced by its top scores in Vegetation Coverage (C1) and Native Plant Proportion (C5), resulting in a high ecological baseline. Conversely, the TPDF site, dedicated to textile printing and dyeing, required vast areas of hardened ground for logistics and wastewater basins, leaving a legacy of low vegetation coverage (C1) and a compromised ecological foundation that hinders natural recovery.

Second, the divergence in Ecological Value (B2) and pollution status is a direct consequence of their production nature. XMF's military-industrial operations involved localized pollution, primarily heavy metals and lubricants (C8), categorizing it as a 'Moderately Polluting Industry'. In contrast, TPDF's use of complex dyes,

auxiliaries, and organic compounds led to widespread and severe contamination, marking it as a 'Heavily Polluting Industry' (C8). This fundamental difference is reflected in their pollution control difficulty scores. Furthermore, XMF's superior performance in 'Connection to Green Spaces' (C7) is not incidental. Its historical placement within a planned industrial zone, often co-located with other large facilities possessing green buffers, enhanced its connectivity to the urban ecological network. TPDF, potentially sited for water access and effluent disposal, ended up in a more isolated location, weakening its ecological linkages.

Third, the assessment of Stormwater Management (B3) further underscores the role of pre-existing site conditions. XMF's higher score (2.29 vs. 1.89 for TPDF) is directly linked to its superior vegetation coverage (C1), which promotes infiltration and retention, despite both sites having generally poor underlying permeability due to historical industrial compaction and construction.

Finally, the chasm in urban integration, captured by the Community Structure (B4) and Service Facilities (B5) criteria, is rooted in their original locational logic and the subsequent urban development patterns. The XMF site, as part of a significant state-owned industrial base, was integrated into a well-serviced urban district from its inception. Over time, the surrounding area developed into mature residential neighborhoods, explaining its high scores for Population Density (C15), Transportation Services (C17), and other public amenities. Its transformation into a park thus serves an immediate and dense population. The TPDF site, typical of industries with specific logistical or environmental needs, was historically situated on the urban fringe. The subsequent pattern of urban growth has not fully integrated this area, leaving it with lower community density and a critical lack of service facilities (B5 score: 3.85 for XMF vs. 1.47 for TPDF), thereby limiting its immediate social demand value and accessibility.

In summary, the quantitative evaluation reveals that the 'hard' military-industrial legacy of XMF conferred a robust ecological and urban-integration advantage. In contrast, the 'soft' but chemically intensive legacy of the textile industry left TPDF with a more deeply impaired ecosystem and a peripheral relationship to the urban fabric, necessitating a fundamentally different regeneration approach.

##### 4.2. Conceptual Differentiated Landscape Optimization Strategies

Based on the above evaluation and comparison, targeted landscape optimization strategies are proposed for the two industrial wasteland sites.

For XMF site, the strategy proposed an ecology- and culture-integrated comprehensive park. First, ecological restoration is prioritized by conserving and enhancing existing vegetation communities to establish a stable near-natural ecosystem. Second, the industrial heritage's value is revitalized through the adaptive reuse of iconic structure into immersive museums, exhibition hall, or

outdoor art spaces, reinforcing its robust military-industrial cultural character. Third, community needs are met by incorporating facilities for leisure, play, and education, culminating in an urban park that blends ecology, culture, and recreation.

For TPDF site, the strategy focuses on zoned remediation to create an art-led green cultural district. First, severely polluted printing and dyeing areas undergo risk-based containment, while less polluted zones receive sensor-guided soil improvement. Second, flexible, low-intervention approaches are adopted: transforming contaminated zones into land art or hardy plant displays, and applying 'light-touch' renovations to retained buildings to attract creative tenants. Third, the site is positioned as a regional fashion art or cultural-creative park with phased integration into the urban fabric or spur local vitality.

To enhance the scientific precision and implementation efficiency of these strategies, an AI-assisted planning workflow is proposed as shown in **Figure 6**, integrating specific technologies into key stages: (1) Site Assessment and Analysis: Machine learning (ML) algorithms are employed for pollution mapping and predicting ecological restoration potential by analyzing spatial data such as soil samples and plant vegetation indices. (2) Conceptual and Generative Design: Using generative design tools (deep learning or optimization algorithms) to automatically generate and evaluate multiple spatial layout options that meet predefined constraints (e.g., sun exposure, landscape connectivity, zoning regulations) and objectives such as preserving heritage structures. (3) Simulation and Optimization: Using deep neural network simulates long-term outcomes such as vegetation community development, stormwater runoff, and human foot traffic patterns under different design scenarios. (4) Monitoring and Management: Using computer vision and internet of things (IoT) sensor networks to monitor soil health, plant growth, and visitor flows, supporting adaptive management post-construction.

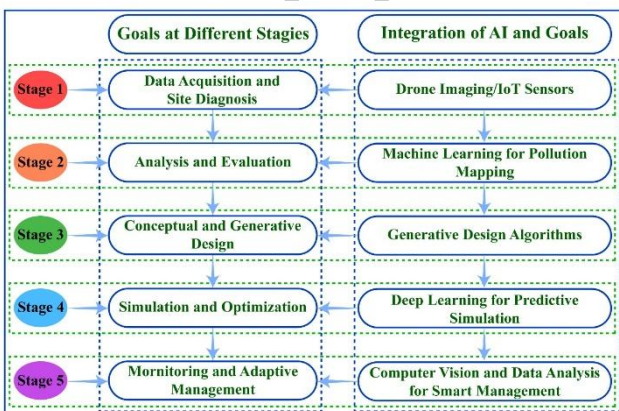


**Figure 6.** Schematic diagram of the AI-assisted workflow for industrial brownfield regeneration planning.

## 5. Conclusion

This study quantitatively evaluated and compared the green value of two typical industrial wastelands, XMF and

TPDF, in Harbin, China. The main conclusions are as follows:

(1) The green value evaluation system developed effectively quantifies the potential of industrial wastelands for transformation into urban green spaces. Significant differences in ecological baselines, pollution levels, and urban integration resulted in XMF (3.76) outperforming TPDF (2.44).

(2) Original industrial attributes critically shape all aspects of green value and must be considered in formulating differentiated regeneration strategies.

(3) The proposed AI-assisted planning workflow, integrating machine learning for contamination mapping, generative design for spatial configuration, and predictive modeling for ecosystem simulation, can significantly improve the feasibility, adaptability, and scientific robustness of such strategies. For XMF, ecological preservation and cultural enhancement are prioritized, while TPDF requires risk control, flexible design, and creativity-driven reactivation.

This research confirms the value of evidence-based and technology-supported landscape design in industrial wasteland regeneration. Future studies should incorporate detailed engineering measures, cost-benefit analysis, and public participation to strengthen strategy implementation.

## Author Contributions

Conceptualization, J.C. (Jian Cui) and Y.Z. (Yuehua Zhang); methodology, J.C. (Jian Cui) and Y.Z. (Yuehua Zhang); software, J.C. (Jian Cui) and Z.J. (Zhenyu Jia); validation, J.C. (Jian Cui) and Y.Z. (Yuehua Zhang); formal analysis, J.C. (Jian Cui) and Z.J. (Zhenyu Jia); investigation, Z.J. (Zhenyu Jia) and Y.Z. (Yuehua Zhang); data curation, J.C. (Jian Cui); writing--original draft preparation, J.C. (Jian Cui); writing--review and editing, Y.Z. (Yuehua Zhang); funding acquisition, Z.J. (Zhenyu Jia) and Y.Z. (Yuehua Zhang). All authors have read and agreed to the published version of the manuscript.

## Data Availability Statement

The data presented in this study are available on request from the corresponding author.

## Acknowledgments

This research has been fully supported by M-Grass Eco. and Environ. Company under the project number 2022RC-High Level-5.

## Conflicts of Interest

The authors declare no conflict of interest.

## References

Accordino, J. and Johnson, G. T. (2000). Addressing the vacant and abandoned property problem. *Journal of Urban Affairs*, 22(3), 301-315. Doi:10.1111/0735-2166.00058.

Adams, D., De Sousa, C., Tiesdell, S. (2010). Brownfield development: A comparison of North American and British approaches. *Urban Studies*, 47(1), 75-104. Doi:10.1177/0042098009346868.

Anderson, E. and C., Minor, E. S. (2017). Vacant lots: An underexplored resource for ecological and social benefits in cities. *Urban Forestry and Urban Greening*, 21, 146-152. Doi:10.1016/j.ufug.2016.11.015.

Akkerman, A., and Cornfeld, A. F. (2009). Greening as an urban design metaphor: Looking for the city's soul in leftover spaces. *The Structurist*, 49(50), 30-35.

Atkinson, G., Doick, K., Birmingham, K., France, C. (2014). Brownfield regeneration to greenspace: Delivery of project objectives for social and environmental gain. *Urban Forestry & Urban Greening*, 13(3), 586-594. Doi:10.1016/j.ufug.2013.04.002.

Barrado, C., Pérez-Batlle, M., Lopez, M., Pastor, E. (2016). Paired T-test analysis to measure the efficiency impact of a flying RPAS in the non-segregated airspace. *2016 IEEE/AIAA 35th Digital Avionics Systems Conference (DASC), Sacramento, CA, USA*, 1-7. Doi: 10.1109/DASC.2016.7778008.

Beam, D. R., Szabo, A., Olson, J., Hoffman, L., Beyer, K. M. M. (2021). Vacant lot to community garden conversion and crime in Milwaukee: A difference-in-differences analysis. *Injury Prevention*, 27(5), 403-408. Doi:10.1136/injuryprev-2020-043767.

Beames, A., Broekx, S., Schneidewind, U., Landuyt, D., van der Meulen, M., Heijungs, R., Seuntjens, P. (2018). Amenity proximity analysis for sustainable brownfield redevelopment planning. *Landscape and Urban Planning*, 171, 68-79. Doi:10.1016/j.landurbplan.2017.12.003.

Byun, D. H. (2001). The AHP approach for selecting an automobile purchase model. *Information & Management*, 38 (5), 289-297. Doi: 10.1016/S0378-7206(00)00071-9

Cady, T. J., Rahn, D. A. Brunsell, N. A., Lyles, W. (2020). Conversion of abandoned property to green space as a strategy to mitigate the urban heat island investigated with numerical simulations. *Journal of Applied Meteorology and Climatology*, 59(11), 1827-1843. Doi:10.1175/JAMC-D-20-0093.1.

Chen, B., Hashimoto, S. (2025). Integrate brownfield greening into urban planning: A review from the perspective of ecosystem services. *Urban Forestry & Urban Greening*, 104, 128642. Doi:10.1016/j.ufug.2024.128642.

Chien, S.-C., Knoble, C. (2024). Uneven burdens: The intersection of brownfields, pollution, and socioeconomic disparities in New Jersey, USA. *Sustainability*, 16(23), 10535. Doi:10.3390/su162310535.

Cui, J., Jensen, S. T., MacDonald, J. (2022). The effects of vacant lot greening and the impact of land use and business presence on crime. *Environment and Planning B: Urban Analytics and City Science*, 49(3), 1147-1158. Doi:10.1177/23998083211050647.

Cui, J.; Sharifi, E.; Bartesaghi Koc, C.; Yi, L.; Hawken, S. (2025). Factors shaping biodiversity in urban voids: A systematic literature review. *Land*, 14, 821. Doi: 10.3390/land14040821.

Cundy, A. B., Bardos, R. P., Puschenreiter, M., Mench, M., Bert, V., Friesl-Hanl, W., Muller, I., Li, X. N., Weyens, N., Witters, N., Vangronsveld, J. (2016). Brownfields to green fields: Realizing wider benefits from practical contaminant phytomanagement strategies. *Journal of Environmental Management*, 184(1), 67-77. Doi:10.1016/j.jenvman.2016.03.028.

Derudder, B. and Taylor, P. J. (2021). Not Chicago: Voids in world city network formation. *Urban Geography*, 42(10), 1500-1524. Doi:10.1080/02723638.2020.1810490.

Draus, P., Haase, D., Napieralski, J., Sparks, A., Qureshi, S., Roddy, J. (2020). Wastelands, greenways and gentrification: Introducing a comparative framework with a focus on Detroit, USA. *Sustainability*, 12(15), 6189. Doi:10.3390/su12156189.

Fu, Q., Han, Y., Xiang, S., Zhu, J., Zhang, L., Zheng, X. (2024). Spatial characteristics of brownfield clusters and city-brown patterns: Case studies of resource-exhausted cities in China. *Land*, 13(8), 1251. Doi:10.3390/land13081251.

Ge, Y.W. (2017). Suggestions on further promoting the construction of Harbin smart city: Based on the investigation of the current situation of Xiangfang District smart city construction. *Decision Consulting*, (3), 16-19. Doi: 10.3969/j.issn.1006-3404.2017.03.007.

Gobster, P. H., Hadavi, S., Rigolon, A., Stewart, W. P. (2020). Measuring landscape change, lot by lot: Greening activity in response to a vacant land reuse program. *Landscape and Urban Planning*, 196, e103729. Doi:10.1016/j.landurbplan.2019.103729.

Hsiao, H. (2022). Spatial distribution of urban gardens on vacant land and rooftops: A case study of 'The Garden City Initiative' in Taipei City, Taiwan. *Urban Geography*, 43(8), 1150-1175. Doi:10.1080/02723638.2021.1901036.

Hwang, S.W. and Lee, S.J. (2019). Unused, underused, and misused: An examination of theories on urban void spaces. *Urban Res. Pract.* 13(5), 540-556. Doi:10.1080/17535069.2019.1634140.

Li, M., Li, R., Liu, X., Fabris, L. M. F. (2024). A brownfield regeneration in urban renewal contexts visual analysis: research hotspots, trends, and global challenges. *Landscape Research*, 49(6), 896-911. Doi:10.1080/01426397.2024.2359521.

Li, Y., Chen, X., Tang, B., Wong, S. (2018). From project to policy: Adaptive reuse and urban industrial land restructuring in Guangzhou city, China. *Cities*, 82, 68-76. Doi:10.1016/j.cities.2018.05.006.

Mao, L., Zheng, Z., Meng, X., Zhou, Y., Zhao, P., Yang, Z., Long, Y. (2022). Large-scale automatic identification of urban vacant land using semantic segmentation of high-resolution remote sensing images. *Landscape and Urban Planning*, 222, e104384. Doi:10.1016/j.landurbplan.2022.104384.

Mo, J.T., Liu, F., Deng, X.X. (2025). A group decision making model with non-reciprocal fuzzy preference relations based on Pearson correlation coefficient. *Expert Systems with Applications*, 276. Doi:10.1016/j.eswa.2025.127095.

Mrak, I., Ambruš, D., Marović, I. (2022). A holistic approach to strategic sustainable development of urban voids as historic urban landscapes from the perspective of urban resilience. *Buildings*, 12(11), 1852. Doi:10.3390/buildings12111852.

Naghibi, M., Faizi, M., Ekhlassi, A. (2021). Design possibilities of leftover spaces as a pocket park in relation to planting enclosure. *Urban Forestry & Urban Greening*, 64, e127273. Doi:10.1016/j.ufug.2021.127273.

Newman, G., Park, Y., Bowman, A. O. M., Lee, R. J. (2018). Vacant urban areas: Causes and interconnected factors. *Cities*, 72(B), 421-429. Doi:10.1016/j.cities.2017.10.005.

Preston, P. D., Dunk, R. M., Smith, G. R., Cavan, G. (2023). Not all brownfields are equal: A typological assessment reveals hidden green space in the city. *Landscape and Urban Planning*, 229, e104590. Doi:10.1016/j.landurbplan.2022.104590.

Preston, P. D., Dunk, R. M., Smith, G. R., Cavan, G. (2024). Examining regulating ecosystem service provision by brownfield and park typologies and their urban distribution. *Urban Forestry & Urban Greening*, 95, 128311. Doi:10.1016/j.ufug.2024.128311.

Qu, Y., Jiang, G., Li, Z., Shang, R., Zhou, D. (2020). Understanding the multidimensional morphological characteristics of urban idle land: Stage, subject, and spatial heterogeneity. *Cities*, 97, e102492. Doi:10.1016/j.cities.2019.102492.

Rupprecht, C. D. D. and Byrne, J. A. (2014). Informal urban greenspace: A typology and trilingual systematic review of its role for urban residents and trends in the literature. *Urban Forestry & Urban Greening*, 13(4), 597-611. Doi:10.1016/j.ufug.2014.09.002.

Song, Y., Lyu, Y., Qian, S., Zhang, X., Lin, H., Wang, S., (2022). Identifying urban candidate brownfield sites using multi-source data: the case of Changchun City, China. *Land Use Policy*, 117. Doi:10.1016/j.landusepol.2022.106084.

Song, X., Wen, M., Shen, Y., Feng, Q., Xiang, J., Zhang, W., Zhao, G., Wu, Z. (2020). Urban vacant land in growing urbanization: An international review. *Journal of Geographical Sciences*, 30(4), 669-687. Doi:10.1007/s11442-020-1749-0.

Stanford, H. R., Hurley, J., Garrard, G. E., Kirk, H. (2025). The contribution of informal green space to urban biodiversity: a city-scale assessment using crowdsourced survey data. *Urban Ecosystems*, 28(1), 1-16. Doi:10.1007/s11252-024-01623-0.

Xi, S. (2024). Transforming urban industrial wastelands using a CNN-based land classification model. *Soft Computing*, 28(2), 903-916. Doi:10.1007/s00500-023-09458-1.

Xu, A.J. and Xu, D.W. (2020). Research on landscape interactivity based on environmental: A case study of Lilac Park in Harbin Qunli New Area. *Modern Horticulture*, 43(9), 184-186. Doi: CNKI:SUN:JXYA.0.2020-09-093

You, H.J. (2024). Research on high quality development strategies for Harbin's ice and snow industry—Against the background of the Harbin Asian Winter Games. *Northern Economy and Trade*, (1), 1-4.

Zhang, B.C., Wang, Q.L., Zhang, H. (2023). Research on the survey and protection strategies of modern railway architectural heritage in Harbin. *Journal of Suzhou University of Science and Technology*, 36(4), 39-43.. Doi:10.3969/j.issn.1672-0679.2023.04.006.

**Supplementary Tables (Note: The meanings of each criteria code in the following tables as shown in Figure 4.)**

**Suppl Table 1.** Summary of expert consultancy panel composition

Professional title	Affiliation	Specialty	Participant count	Inquiry method
Professor	Northeast Agricultural University	Landscape architecture	3	Field visit and investigation
Professor	Northeast Forestry University	Landscape architecture	3	Field visit and investigation
Professor	Harbin Institute of Technology	Landscape architecture	2	Field visit and investigation
Professor	Heilongjiang Agricultural Vocational Engineering College	Architectural engineering	2	Field visit and investigation
Associate professor	Heilongjiang Vocational & Technical University of Agricultural Engineering	Landscape architecture	1	Field visit and investigation
Associate professor	Heilongjiang College of Architectural Technology	Urban Architecture	2	Field visit and investigation
Urban designer	Heilongjiang Building Design Institute	Landscape architecture	1	Field visit and investigation
Manager	Harbin Sanfeng			
Landscape Co., Ltd	Landscape architecture	1	Field visit and investigation	

**Suppl Table 2.** Weight and ranking of sub-criteria in the eco-quality (B1) dimension

Sub-criteria	C1	C2	C3	C4	C5	Wi	Order
C1	1	7.0613	3.8602	5.9636	0.8624	0.3573	2
C2	0.1416	1	0.2142	0.3618	0.1836	0.0429	5
C3	0.2591	4.7619	1	4.7141	0.2604	0.1563	3
C4	0.1678	2.7778	0.2123	1	0.1421	0.0651	4
C5	1.1628	5.5556	3.8462	7.1429	1	0.3784	1

**Suppl Table 3.** Weight and ranking of sub-criteria in the ecological value (B2) dimension

Sub-criteria	C6	C7	C8	C9	Wi	Order
C6	1	1.0624	4.9136	4.3478	0.3973	2
C7	0.9434	1	5.8747	5.5556	0.4274	1
C8	0.2037	0.1704	1	2.4391	0.1053	3
C9	0.2312	0.18	0.41	1	0.0700	4

**Suppl Table 4.** Weight and ranking of sub-criteria in stormwater management (B3) dimensions

Sub-criteria	C10	C11	C12	Wi	Order

C10	1	4.8208	2.9614	0.6456	1
C11	0.2075	1	0.5733	0.1307	3
C12	0.3378	1.7544	1	0.2237	2

**Suppl Table 5.** Weights and ranking of sub-criteria in the community structure (B4) dimension

Sub-criteria	C13	C14	C15	C16	Wi	Order
C13	1	6.8124	1.7802	2.9342	0.4739	1
C14	0.1468	1	0.2641	0.4186	0.0688	4
C15	0.5618	3.8462	1	3.0616	0.3144	2
C16	0.3413	2.439	0.3268	1	0.1429	3

**Suppl Table 6.** Weights and ranking of sub-criteria in the service facilities (B5) dimension

Sub-criteria	C17	C18	C19	C20	C21	Wi	Order
C17	1	5.0283	4.9321	3.8849	2.7654	0.4667	1
C18	0.1992	1	3.0633	1.8911	1.1228	0.1631	2
C19	0.2028	0.3268	1	0.2942	0.2214	0.0541	5
C20	0.2577	0.5291	3.4483	1	1.9862	0.1621	3
C21	0.3623	0.8929	4.5455	0.5051	1	0.1539	4